Journal Pre-proof

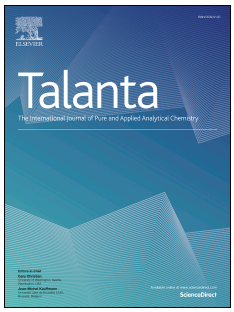

Development of an electrochemical sensor using carbon nanotubes and hydrophobic natural deep eutectic solvents for the detection of α-glucosidase activity in extracts of autochthonous medicinal plants

Nicolás A. Aschemacher, Carla M. Teglia, Álvaro S. Siano, Fabiana A. Gutierrez, Héctor C. Goicoechea

PII: S0039-9140(23)01064-0

DOI: https://doi.org/10.1016/j.talanta.2023.125313

Reference: TAL 125313

To appear in: *Talanta*

Received Date: 24 August 2023

Revised Date: 11 October 2023

Accepted Date: 13 October 2023

Please cite this article as: Nicolá.A. Aschemacher, C.M. Teglia, Á.S. Siano, F.A. Gutierrez, Hé.C. Goicoechea, Development of an electrochemical sensor using carbon nanotubes and hydrophobic natural deep eutectic solvents for the detection of α-glucosidase activity in extracts of autochthonous medicinal plants, *Talanta* (2023), doi: https://doi.org/10.1016/j.talanta.2023.125313.

This is a PDF file of an article that has undergone enhancements after acceptance, such as the addition of a cover page and metadata, and formatting for readability, but it is not yet the definitive version of record. This version will undergo additional copyediting, typesetting and review before it is published in its final form, but we are providing this version to give early visibility of the article. Please note that, during the production process, errors may be discovered which could affect the content, and all legal disclaimers that apply to the journal pertain.

© 2023 Published by Elsevier B.V.

Nicolás A. Aschemacher: Conceptualization, Methodology, Validation, Investigation

Carla M. Teglia: Conceptualization, Methodology, Validation, Visualization, Writing - Original Draft, Investigation, Funding acquisition

Álvaro S. Siano: Investigation, Writing - Review & Editing

Fabiana A. Gutierrez: Conceptualization, Methodology, Validation, Writing - Original Draft, Investigation, Funding acquisition

Héctor C. Goicoechea: Conceptualization, Writing - Review & Editing, Funding acquisition

Journal Pre-proof

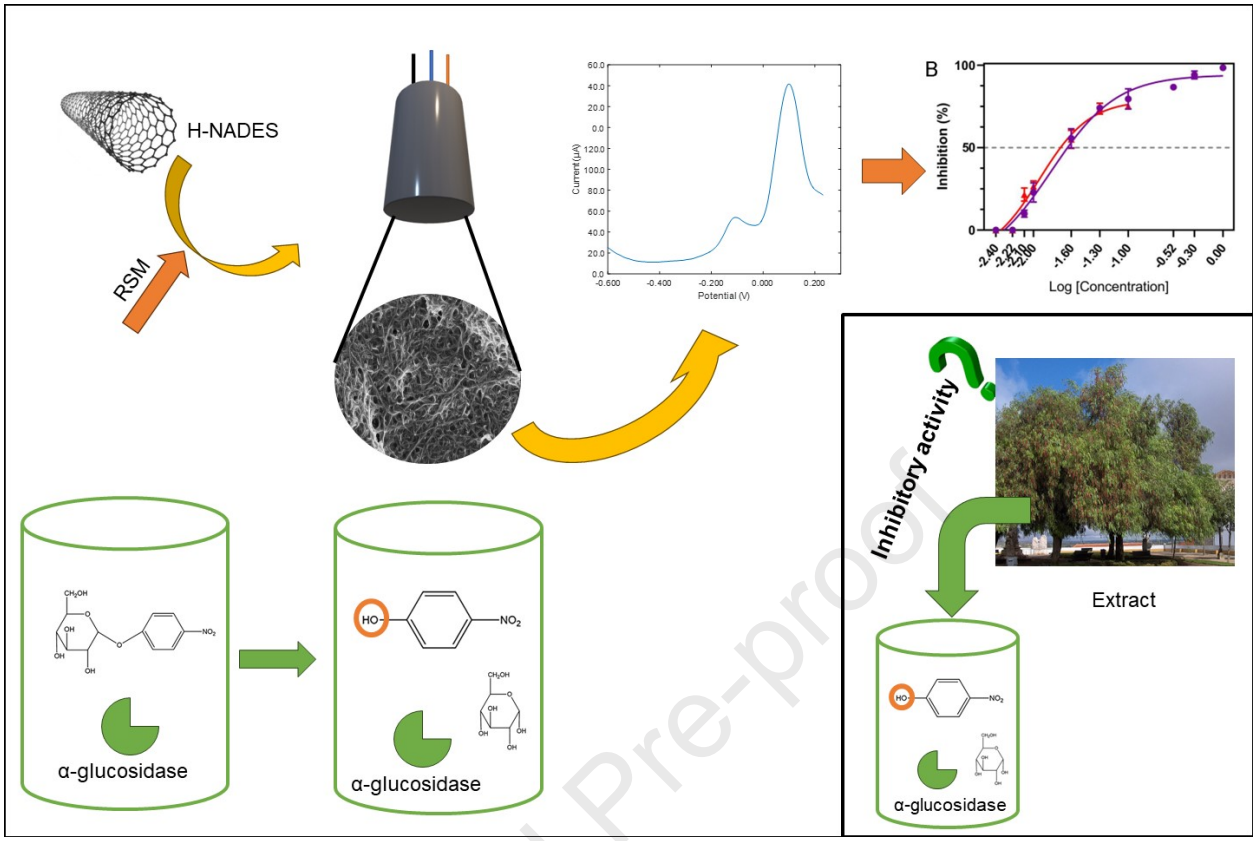

Journal Pre-proof

Journal Pre-proof

Development of an electrochemical sensor using carbon nanotubes and hydrophobic natural deep eutectic solvents for the detection of α-glucosidase activity in extracts of autochthonous medicinal plants

Nicolás A. Aschemacher[a,b], Carla M. Teglia[a,c], Álvaro S. Siano[b,c], Fabiana A. Gutierrez[a,c,*], Héctor C. Goicoechea[a,c]

[a]*Laboratorio de Desarrollo Analítico y Quimiometría (LADAQ), Cátedra de Química Analítica I, Facultad de Bioquímica y Ciencias Biológicas, Universidad Nacional del Litoral, Ciudad Universitaria, 3000, Santa Fe, Argentina.*

[b]*Laboratorio de Péptidos Bioactivos (LPB), Departamento de Química Orgánica, Facultad de Bioquímica y Ciencias Biológicas, Universidad Nacional del Litoral, Ciudad Universitaria, 3000, Santa Fe, Argentina*

[c]*Consejo Nacional de Investigaciones Científicas y Técnicas (CONICET), Godoy Cruz 2290 CP C1425FQB, Buenos Aires, Argentina*

*To whom correspondence should be addressed: E-mails: fabigutierrez@gmail.com

Journal Pre-proof

Journal Pre-proof

Abstract

The present work describes for the first time the use of a hydrophobic natural deep eutectic solvent (H-NADES) as a dispersant for carboxylated nanotubes for the design and construction of an electrochemical sensor for the assay of α-glucosidase and its inhibitors. In this work, we used as the electrochemical probe the product of the enzymatic reaction, which consists of two redox groups and generates the analytical signal. The combination of de carboxylic multi-walled carbon nanotubes (MWCNTc) and the H-NADES of thymol and lactic acid (TLa) increases the electroactive surface area and promotes electron transfer of the electrode modified with carbon nanotubes. The electrochemical sensor enabled the detection of α-glucosidase in a range of 0.004-0.1 U mL^{-1} with a detection limit of 0.0013 U mL^{-1}, which is lower than most existing methods. In addition, two α-glucosidase inhibitors, acarbose and quercetin, and two plant extracts, *Schinus molle* and *Eugenia uniflora*, were evaluated to assess the feasibility of screening potential antidiabetic drugs, and the IC50 values were 5.37 µg mL^{-1} and 5.28 µg mL^{-1}. Thus, this sensing strategy represents the beginning of the incorporation of NADES in the development and design of novel sensors and their application in electrochemistry and medical analysis.

Keywords: carbon nanotubes; response surface methodology; electrochemical sensors; H-NADES; α-glucosidase; medicinal plants

Journal Pre-proof

Journal Pre-proof

1. Introduction

Since the 12th century, type 2 diabetes mellitus (T2DM) has become one of the major global health emergencies [1]. T2DM is a metabolic disorder characterized by high blood glucose levels due to impaired insulin secretion by the pancreas [2]. It is estimated that approximately 425 million people (20-79 years of age) worldwide suffer from T2DM, and ~~it~~ this number is predicted to increase to approximately 629 million by 2045 [1].

The enzyme α-glucosidase is considered a therapeutic target for the treatment of T2DM because it plays an important role in carbohydrate metabolism [3-5]; it converts starch and disaccharides into absorbable monosaccharides such as glucose, which is why it is responsible for the increase in blood glucose levels [6]. Inhibition of this enzyme could slow carbohydrate digestion and ultimately the absorption of monosaccharides, leading to a decrease in postprandial plasma glucose levels [7].

Two main methods can be used to determine α-glucosidase activity: an animal model for *in vivo* screening and an enzyme inhibitor model for *in vitro* screening [8, 9]. However, *in vivo* screening involves lengthy experiments and high costs, whereas the model of enzyme inhibition based on the use of para-nitrophenyl-α-D-glucopyranoside (*p*-NPG) as a substrate has limited sensitivity, since the activity of α-glucosidase inhibitors is usually quantified by measuring the absorbance of 4-nitrophenol (*p*-NP) released by *p*-NPG at 400 nm [10], so, in certain cases, the absorbance of the inhibitor may coincide with that of *p*-NP, directly affecting the measured value [11].

To overcome the drawbacks of the above methods, many efforts have been made to detect the activity of this enzyme by fluorescence [12] and electrochemistry [5, 13-16]. Remarkably, the development of an electrochemical method is characterized by its high sensitivity and ease of use, and has attracted much attention in the field of detection of α-glucosidase activity. However, most of the available electrochemical sensors are not reusable, which limits their

application. Therefore, it is very important to develop a reusable, sensitive, and effective method to detect enzyme activity in order to develop new and more effective α-glucosidase inhibitors.

During the development of an electrochemical method, several authors have proposed different ways to modify the composition of bare carbon paste electrodes (CPGEs) to improve their electrochemical properties [17, 18]. Carbon nanotubes (CNTs) are the most commonly used materials in electrochemical sensors due to their high conductivity, chemical stability, flexibility, and low-cost [19]. However, one of the most common problems limiting their application is the agglomeration of these nanomaterials [20]. Therefore, good dispersibility of CNTs can be achieved by chemical functionalization, e.g., with -COOH [21], -OH [22], and -NH_2 [23], with the addition of a suitable solvent to obtain a stable and homogeneous dispersion.

According to the principles of green analytical chemistry (GAC) [24], the use of conventional solvents must be reduced. In this scenario, the use of natural deep eutectic solvents (NADES) appears as a green alternative–because their components are natural metabolites such as organic acids, sugars, amino acids, sugars, alcohols, and amines with different groups capable of intermolecular interactions; they form when hydrogen bond acceptor and hydrogen bond donor compounds are mixed at graded temperatures with constant stirring. There are hydrophobic NADES (H-NADES) in which the predominant driving forces are the π-π interactions between aromatic rings [25]. In contrast to hydrophilic NADES, H-NADES exhibit lower viscosity because the Coulombic charge interactions are omitted [26].

Few works describe the use of NADES in electrochemistry, as a supporting electrolyte [27, 28], to form a composite [29], to generate biopolymer electrolytes [30], and as conducting ligands for glassy carbon electrode (GCE) modification, due to their attractive properties, including good conductivity, low vapor pressure, and high chemical stability [31] .

The use of the chemometric tool allows the researcher to find the optimal experimental conditions and reduce the number of experiments [32]. In the field of electrochemistry, this tool is not yet regularly used, which means that the possibility of founding the best experimental combination of factor is lost. In the present work, the combination of electrochemical methods and chemometric tools was used to optimize the dispersion and measurement conditions.

In this work, the properties of H-NADES as a dispersant CNT-COOH were analyzed for the first time. Moreover, this is the first time that a NADES has been used for enzymatic determination. This novel platform was used to determine *p*-NP, the product released by the enzymatic action of α-glucosidase, by differential pulse voltammetry (DPV). This sensor is ideal for the simple and rapid search for enzyme inhibitors in extracts from various plant species.

2. Material and method

2.1. Reagents

Carboxylic Multi-walled carbon nanotubes (MWCNTc) were supplied from Dropsens. Lactic acid, thymol, *p*-nitro phenol (*p*-NP), NaH_2PO_4, Na_2HPO_4 and ethanol (EtOH) were purchased from Cicarelli (San Lorenzo, Argentina). Acarbose, *p*-nitrophenyl α-D-glucopyranoside (*p*-NPG) and α-Glucosidase from *Saccharomyces cerevisiae* were purchased from Sigma (Sigma–Aldrich Inc, St Louis, USA). Phosphate buffer solution (PB) 0.100 M pH 6.8 was employed as supporting electrolytes. All the experiments were conducted at room temperature. Ultrapure water (ρ = 18 MΩ cm) from a Millipore-MilliQ system was used for preparing all the solutions.

2.2. Preparation of hydrophobic natural deep eutectic solvent (H-NADES)

The H-NADES was prepared following the recommendation of Dazat et al. [33]. Briefly, the component of the H-NADES, thymol and lactic acid (TLa), were placed into a glass baker at a molar ratio of 1:2, respectively. The baker was heated at 60 °C under magnetic stirring at 250 rpm until the crystal disappeared and continued stirring for another 15 min.

2.2. Apparatus and software

The electrochemical measurements were performed with an μStat-i 400s potentiostat Metrohm DropSen (Asturias, España). The electrodes were inserted into the cell (BAS, Model MF-1084) through holes in its Teflon cover. A platinum wire and Ag/AgCl, 3 M NaCl (BASI, Model RE-5B) were used as counter and reference electrodes, respectively. All potentials are referred to as the reference electrode. Sonication treatments were carried out either with an ultrasonic bath (TESTLAB, model TB04) of 40 kHz frequency and 160 W of nominal power.

UV-Vis experiments were performed with a Lambda UV-Vis spectrometer (Perkin Elmer, Massachusetts, U.S.A.). Sonication treatments were carried out either with an ultrasonic bath (TESTLAB, model TB04) of 40 kHz frequency and 160 W of nominal power.

For the extract concentration, a Rotavapor BÜCHI Labortechnik R-114 (Flawil, Switzerland) was used.

The experimental design building and the posterior analysis were carried out by Design Expert 8.0.0.

For the spectrophotometric enzyme assays, a 96-well microplate reader at 405 nm by microplate reader (Thermo Fisher FC Multiskan) was usedThe IC50 was calculated with a four-parameter logistic curve estimated using Graph Pad Prism 8.0.1 The samples were examined with a Scanning Electron Microscope, Zeiss brand, CrossBeam 350 model. Observations were made under secondary electron imaging mode using an accelerating voltage of 2 kV.

2.3. Experimental design and statistical analysis

2.3.1. Central composite design (CCD) for the sensor optimization

In optimizing the sensor, a ½-fraction CCD was created with five factors and 30 experimental runs (see Table SM1). The factors affecting the design of the sensor were analyzed together,on the one hand (A) the mass of nanotubes between 0.1 –1.0 mg, (B) the percentage of TLa between 2.5 – 15.0% and the sonication time between 5.0 – 30.0 min, and on the other hand the factors of electropolymerization, (D) the accumulation time between 10 – 120 sec and the potential between –1.0 to –0.5 V were analyzed together. The values of each factor correspond to the construction entering the factor range with respect to alpha. Finally, a ½-turn two-block design ($\alpha = 2$) was created with 2 central points per block. The response analyzed was the peak current.

2.3.2. One-factor design for the optimum incubation time optimization

To define the optimum incubation time, a one-factor design was built. Table SM2 shows the eight experimental times analyzed. As response, the peak current was analyzed.

2.4. Preparation of the dispersions

The dispersion was prepared by weighing 0.300 mg $MWCNT_c$ and adding 2.5% of TLa in 1 mL of ethanol, followed by 10 minutes of sonication. Control dispersions were prepared by a similar procedure, i.e., a dispersion of 0.300 mg $MWCNT_c$ to in 1 mL ethanol and 2.5% of TLa in 1 mL ethanol, both sonicated for 10 minutes.

2.5. Preparation of GCE modified with the dispersions

Before modification, the GCEs were polished with alumina slurries of 1.0, 0.30, and 0.05 µm for 2 minutes each. Then, the GCEs were modified by dropping 20 µL of the TLa-

Journal Pre-proof

MWCNT$_c$ dispersion onto the surfaces followed by evaporation of the solvent at room temperature (TLa-MWCNT$_c$/GCE). A similar protocol was used to prepare GCEs modified with MWCNT$_c$ (MWCNT$_c$/GCE) and HNADES (TLa/GCE) using the dispersion described above.

2.6. Standard solutions

Stock solutions were prepared individually with a mass of 10.32 mg acarbose, 4.83 mg quercetin, 1.5 mg *p*-NPG, and 0.69 mg *p*-NP and diluted in 1.00 mL BP 0.100 M pH 6.8 to obtain concentrations of 16 mM for acarbose and quercetin and 5 mM for *p*-NPG and *p*-NP. In addition, the enzyme stock solution was prepared with a mass of 0.4 mg α-glucosidase enzyme and diluted in 2.00 mL BP 0.100 M pH 6.8 to obtain 6.2 U mL^{-1}.

During the experimental period, the stock solution of *p*-NP and *p*-NPG was prepared every day.

2.7. Procedure

Electrochemical experiments were performed in PB. Voltammetric profiles were recorded at 0.100 V s^{-1} cyclic voltammetry (CV).

DPV parameters were as follows: pulse height of 0.004 V, pulse amplitude of 0.050 V, period of 200 ms, and potential range between –0.6V and 0.3 V. The voltammetric profiles shown were obtained after subtracting background currents. All measurements were performed at room temperature.

2.8. α-Glucosidase activity assay.

The assay for α-glucosidase activity was performed by measuring different concentrations of the enzyme at a fixed concentration of the substrate. The different concentrations of α-

188 glucosidase were prepared by dissolving the stock concentration of 6.20 U mL^{-1} with 0.100 M
189 PBS (pH = 6.8). 40.0 μL of 5.00 mM *p*-NPG was added into different concentration of α-
190 glucosidase to form a total volume of 200 μL for the reaction system generating a final
191 concentration of α-glucosidase and *p*-NPG of 0.004, 0.006, 0.008, 0.010, 0.025, 0.050, 0.100,
192 0.200, 0.400, 0.600 and 0.800 U mL^{-1} and 1.00 mM, respectively.

193 Then the resulting mixture was incubated for 20 min at 37 °C. Subsequently, the DPV from
194 −0.6 V to 0.5 V was conducted in the reaction solution. During the detection, two oxidation
195 peaks associated with the oxidation of the nitro group and hydroxyl group coming from *p*-NPG
196 (before and after enzymatic hydrolysis, respectively) were recorded on the TLa-
197 MWCNTc/GCE.

198 To verify the feasibility of the development method, the reference method
199 (spectrophotometric enzyme assays) was carried out in the same conditions of concentrations
200 and incubation time.

201

202 *2.9. Screening of α-glucosidase inhibitors.*

203 As a proof of concept, the inhibitory efficiency of a variety of compounds was performed:
204 acarbose and quercetin.

205 The acarbose was selected due to is a common anti-diabetes drug and the quercetin was
206 selected following the bibliography [34]. The inhibition assay was performed with the different
207 concentration of acarbose and quercetin (8.0, 4.0, 3.0, 2.0, 1.0, 0.50, 0.30, 0.10, 0.05, 0.025,
208 0.01, 0.008, 0.006 and 0.004 mM) and a fixed concentration of enzyme and substrate. The
209 procedure was followed, firstly different volumes of acarbose and quercetin stock solution (16
210 mM) were added to obtain different concentrations (0.004 to 8 mM), mixed with 20 μL of α-
211 glucosidase. After mixture pre-incubation (15 min at 37◦C), 40 μL of *p*-NPG was added into
212 the mixed solution to form a total volume of 200 μL reaction system.

As result, the final concentration of *p*-NPG and α-glucosidase were 1.00 mM and 0.05 U mL^{-1}, respectively. Subsequently, the resulting mixture was incubated for 20 min at 37◦C. Finally, the electrochemical response was recorded by DPV in a potential range of −0.6 to 0.5 V. Subsequently biosensing method was also applied to evaluate the inhibition efficiency of different vegetable extracts.

The inhibitory ratio (%) of acarbose and vegetable extracts with α-glucosidase was calculated as follows:

$$\text{Inhibitory ratio (\%)} = \frac{(I-I^*)}{(I)} \times 100\% \quad (1)$$

where I was the oxidation current from the hydroxyl group in the presence of α-glucosidase and substrate alone, I^* was the oxidation current from the hydroxyl group in the presence of α-glucosidase, substrate and inhibitor.

2.10. In vitro α-glucosidase inhibitory assay

α-Glucosidase inhibitory activities were determined using a 96-well microtiter plate with p-nitrophenyl-α-D-glucopyranoside (PNPG) as the substrate following a slightly modified method described by Feng et al. [35]. Briefly, 20 µL of the enzyme solution (0.5 U mL^{-1} α-glucosidase in PB) and 80 µL of the sample solution were mixed, and preincubated at 37 °C before the initiation of the reaction by adding the substrate. After pre-incubation (15 min), the *p*-NPG solution (40 µL) (5.0 mM *p*-NPG in PB) was added and then incubated at 37 °C for another 20 min in a final volume of 200 µL. The amount of *p*-NP released was quantified at 405 nm and compared to a control which had 80 µl of PB in place of the extract. The α-glucosidase inhibitory activity was expressed as inhibition % and was calculated as follows:

$$\text{Inhibition (\%)} = \left[Abs_{Control} - \left(Abs_{Sample} - B_{Sample} \right) \Big/ Abs_{Control} \right] * 100 \quad (2)$$

where $Abs_{Control}$ is the absorbance of the plate of the control sample, i.e., without inhibitor, Abs_{Sample} is the absorbance of each sample plate, i.e., sample plus inhibitor plus substrate plus enzyme and B_{Sample} is absorbance of the inhibitor control, i.e., inhibitor plus PB.

2.11. Analytical parameters

To define the linear range and the limits of detection (LOD) and quantification (LOQ), according to the recommendation of Gegenschatz et al [36], a calibration curve of 11 point at 0.004 to 0.8 U mL^{-1} by triplicated were established.

2.12. Preparation of herbal plant extracts

Schinus molle (Aguaribay) and *Eugenia uniflora* (Ñangapirí) plant leaves were collected from the Rural Extension Agency of the National Institute of Agricultural Technology in Ángel Gallardo, Santa Fe, Argentina (31.55°S, 60.68°W). The plant leaves were washed and dried in a circulating air oven at 60 °C for 3 hours and subsequently ground by using a mill. The Soxhlet extraction method was used for preparation of aqueous plant extracts. In this method, about 2.0 g of powder was extracted with 210 ml of ultrapure water. The extract was concentrated to dryness under a controlled temperature 30-35°C by making use of a Rotavapor and preserved in a refrigerator till further use.

The stock solutions of the plant extracts were prepared dissolving 1.00 mg in 1.00 ml of PB.

3. Results and Discussion

3.1. Optimization of the experimental parameters

261 *3.1.1. Optimization of the sensor development*

262 After the building of the experimental design, some experiments were carried out (data not
263 shown) to define the values of the factors and the characteristics of the system, e.g., the need
264 to accumulate or not.

265 According to the analysis, the model that best describes the least squares response (LS) is
266 the linear model with double interaction (2FI). As a result, the model was significant (*p*-value
267 < 0.0001) and with non-significant lack of fit (*p*-value 0.1012), demonstrating the goodness of
268 the model. In addition, the R^2 and R^2_{adj} show acceptable results (0.700 and 0.615, respectively).
269 In the optimization, the response was maximized, and the best combination corresponds to
270 0.300 mg MWCNTs, 2.5% TLa, 10 min sonication, 30 sec of accumulation at a potential of –
271 0.60 V. Figure 1 shows the response surface plot corresponding to the TLa% *vs* potential, where
272 the value of the other factors was set to the optimal combination.

Journal Pre-proof

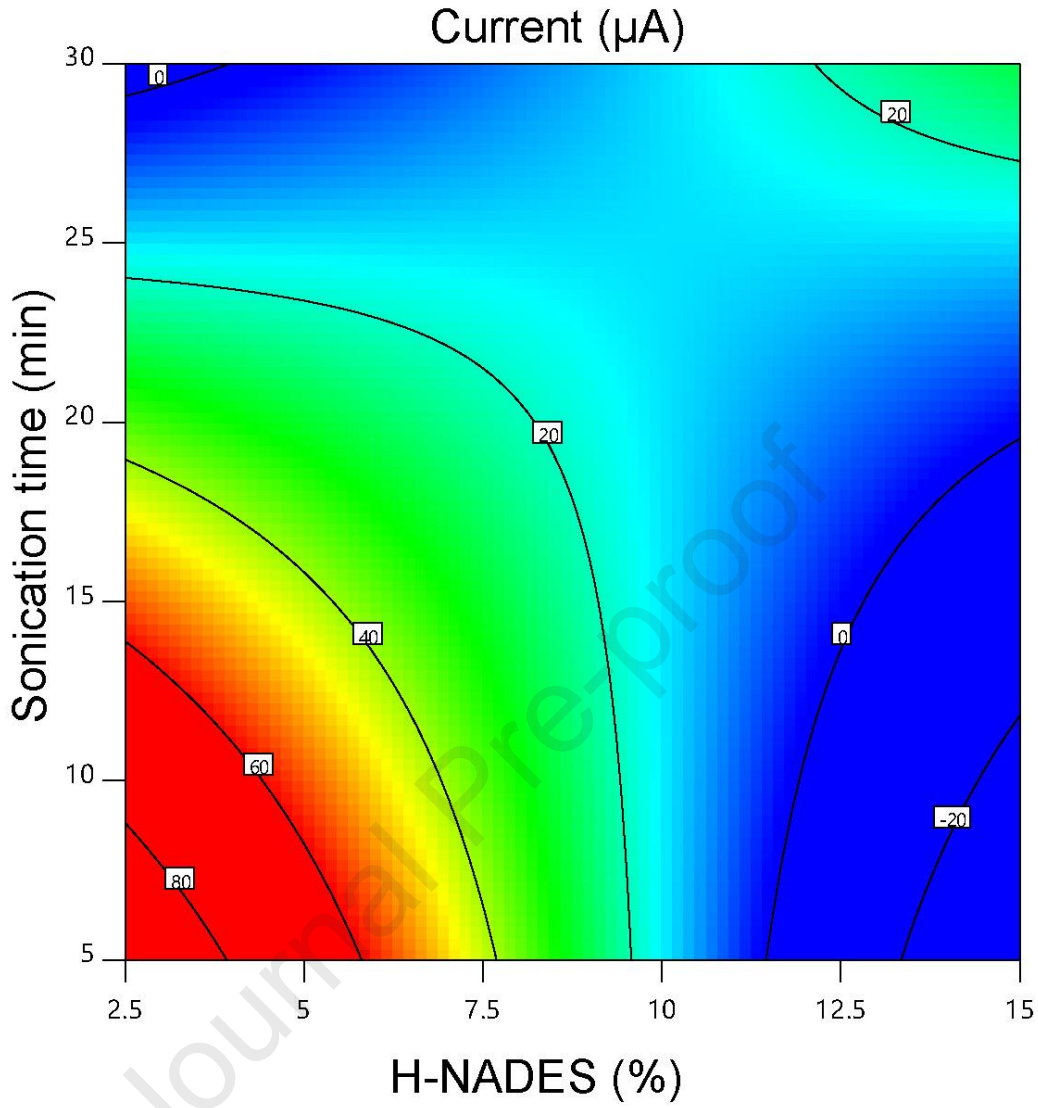

Figure 1. Response surface countour plot for the combined central composite design (CCD). The plot described the %H-NADES vs Potential when the other parameters are fixed at the optimum conditions.

3.1.2. Optimization of the incubation time

A one factor design was built to define the best incubation time. After the analysis, a cubic model resulted significant (*p*-value = 0.0007) with a non-significant lack of fit probability (*p*-value 0.3825). During the optimization step, the incubation time was minimized, and the response was maximized, resulting in a final incubation time of 20.0 min.

3.2. Characterization of TLa-MWCNTc/GCE dispersion

3.2.1. Electrochemical behavior of the modified electrode TLa-MWCNT$_c$/GCE

To evaluate the electrochemical behavior of the TLa-MWCNTc/GCE, *p*-NP and *p*-NPG before and after enzymatic hydrolysis was used. Experiments were performed using CV with a potential range of 0.9 to −1.2 V in 0.100 M PB (pH = 6.75). As shown in Fig. SM1, the CV correspond to *p*-NPG (1.0 mM), *p*-NPG (1.0 mM) with α-glucosidase (0.050 U mL^{-1}) after enzymatic hydrolysis and *p*-NP (1.0 mM).

On the TLa-MWCNTc/GCE, is observed the presence of an oxidation peak of *p*-NPG in the absence of α-glucosidase at −0.09 V (red dotted line), which is associated with the oxidation of the nitro group; in green line, two peaks are observed, the first at −0.09 V corresponding to the oxidation of the nitro group, which occurs both before and after the hydrolysis of *p*-NPG by α-glucosidase. In addition, in the CV of *p*-NPG after the addition of α-glucosidase (green line), a new oxidation peak at 0.1 V appears, which corresponds to the oxidation of the hydroxyl group resulting from the *p*-NPG being hydrolyzed by α-glucosidase. The curve blue dash-dotted line shows the voltammetric profile corresponding to *p*-NP. Two anodic current peaks are observed associated with the oxidation of the nitro group at −0.09 V, which occurs at the same potential as for *p*-NPG, and a second anodic process associated with the oxidation of the hydroxyl group at 0.1 V. The oxidation peaks of *p*-NP and *p*-NPG with α-glucosidase after enzymatic hydrolysis are electrochemically separated on TLa-MWCNTc/GCE, therefore, this surface can serve as an efficient platform to study the enzyme activity of α-glucosidase and the capacity inhibitory of different plant extracts.

For this reason, *p*-NP was used as an electrochemical probe for the following studies related to the optimization of the final sensor.

Journal Pre-proof

p-NPG is hydrolyzed by α-glucosidase enzyme in the presence of PB solution (pH 6.8) to release *p*-NP as can be seen in Fig. 2A [37], due α-glucosidase can cleave specifically α-1,4 glycosidic bonds, resulting in the removal of glucose unit.

The DPVs were carried out on PB containing 1.0 mM *p*-NP in a potential range of −0.4 V to 0.3 V. The arisen oxidation peak at −0.1 V corresponds to the oxidation of the nitro group and the peak that appears at 0.1 V is the oxidation of the hydroxyl group of the *p*-NP (Fig. 2B. Right inset).

The electrochemistry properties of the different sensor platforms were characterized by DPV. Figure 2B depicts the voltammetric profiles for GCE (blue curve), TLa/GCE (orange curve), MWCNTc/GCE (red curve) and TLa-MWCNTc/GCE (violet curve) using 1.0 10^{-3} M *p*-NP as probe. In the right inset, the voltammetric profile (DPV) obtained before subtracting background currents is shown. Comparatively, to evaluate the electrochemical behavior of the different sensor platforms, the peak at 0.1 V is shown, which corresponds to the hydroxyl group oxidation, which was later used as a redox signal to follow the enzymatic reaction, since it is the same potential oxidation peak of *p*-NP oxidation peak of nitro group and hydroxyl group.

Journal Pre-proof

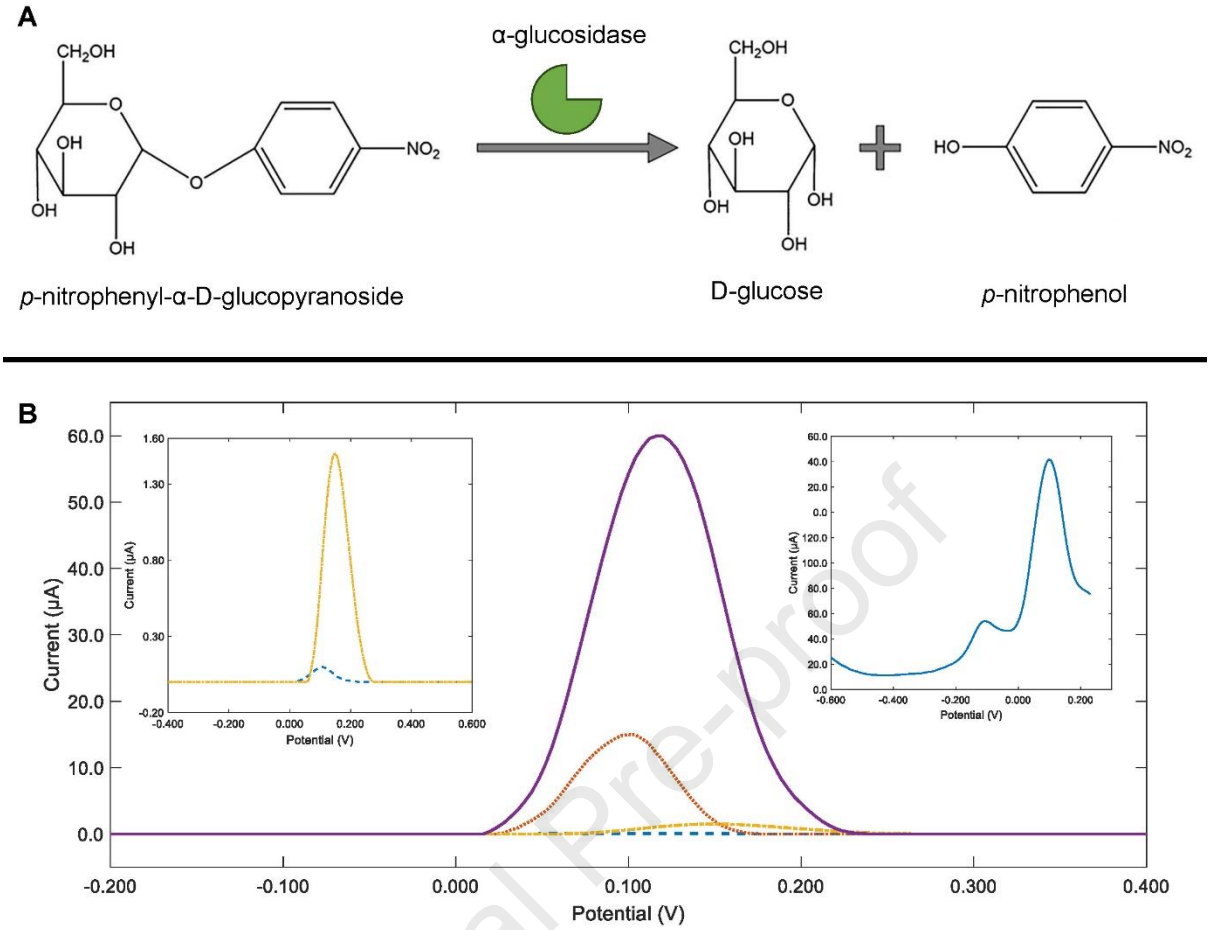

Figure 2. A) Reaction scheme of hydrolysis of colourless p-nitrophenyl-α-d-glucopyranoside to coloured p-nitrophenol by α-glucosidase. B) Differential pulse voltammograms of 1.00 mM *p*-NP in 0.100 M PB (pH = 6.8) on the GCE (blue dotted line), TLa/GCE (yellow dash-dotted line) MWCNTc/GCE (red dots) and TLa-MWCNTc/GCE (violet solid line). Right inset: shown the voltammetric profile (DPV) obtained before subtracting background currents. Left insert: the DPVs of GCE (blue dotted line), and MWCNTc/GCE (yellow dash-dotted line) were magnified. Potential range of −0.4 V to 0.3 V. The voltammetric profiles were obtained after subtracting background currents.

Figure 3 shows the variation of the potential and current of the peak associated with the hydroxyl group. When the GCE surface is modified, the peak current increases, being 15, 150 and 600 times higher for TLa/GCE, MWCNTc/GCE and TLa-MWCNTc/GCE respectively. Regarding the peak potential, a slight shift to more positive potential is observed when GCE is modified with TLa, than when GCE is modified with CNTs (MWCNTc/GCE), which has a lower overpotential than GCE. Moreover, when TLa and CNTs are incorporated into the platform (TLa-MWCNTc/GCE) a shift to more positive potential is again observed than

MWCNTc/GCE, but less than when it is only modified whit TLa. When TLa is present, an increase in oxidation potential is observed, indicating that the hydrophobic nature of NADES slows down electron transfer. Therefore, this suggests that CNTs are the main responsible for the improvement in electron transfer. In the case of TLa-MWCNTc/GCE, an increase in the *p*-NP oxidation current of 4 and 40 times greater than for MWCNTc/GCE and TLa/GCE is observed, clearly showing a synergistic effect between CNT and TLa, which may be due to the fact that the TLa allowed a better dispersion of the carbon nanotubes and therefore increased their electroactive area supports CNTs, clearly showing the importance of H-NADES as a dispersing agent for MWCNTc, since the predominant driving forces are the π-π interactions [22] between aromatic rings between H-NADES and CNTs, in addition to the hydrophobic interactions that make them excellent candidates for the generation of dispersions of different carbon nanomaterials. These results suggest that TLa-MWCNTc not only enlarges the electroactive surface area of the electrode, but also promotes the electron transfer.

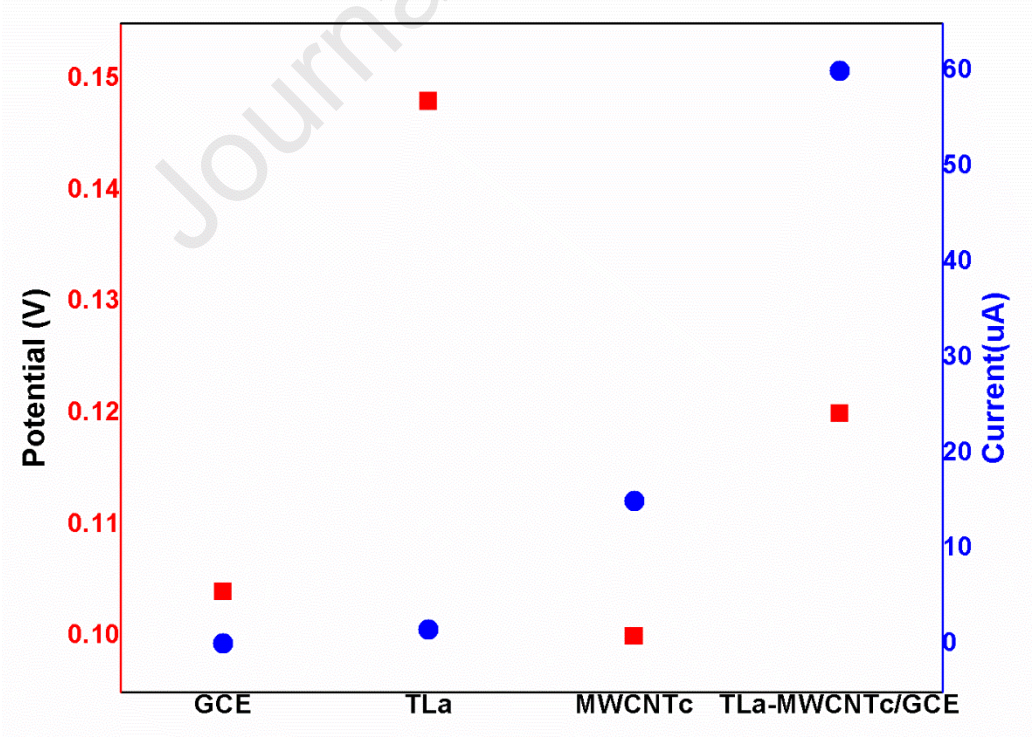

Figure 3. Shows the variation of the potential and current of the peak associated with the oxidation of the hydroxyl group of the *p*-NP generated on different surfaces, GCE, TLa/GCE, MWCNTc/GCE and TLa-MWCNTc/GCE

3.2.2. Effect of scan rate

Figure SM2 shows the effect of different scan rates on the peak oxidation current of *p*-NP on TLa-MWCNTc/GCE using VC. The intensity of the anodic currents increased with the increase of the scan rate (from 10–200 mV s^{-1}), and the potential of the oxidation peaks shifted positively. The linear relationship between oxidation peak currents of *p*-NP and the scan rate was observed in the inset of Fig. SM2 and the linear regression equation can be expressed as follow: $y = 21.119 + 1808.854\,x$ with R^2=0.998. These results are indicative that the electrooxidation of *p*-NP on TLa-MWCNTc/GCE is an adsorptive process.

3.2.3. Accumulation

Since *p*-NP shows that the redox processes on the modified electrode surface are controlled by adsorption, the accumulation conditions on TLa-MWCNTc/GCE were studied to optimize the sensor by experimental design. Subsequently, the DPV with potential from −0.6 V to 0.3 V was conducted in the reaction solution (see Figure SM3) without accumulation (blue dotted line) and accumulated under optimal conditions (red line). It can be seen that the peak currents at 0.1 V, increase by 2.5 times after accumulation compared to the peak currents without prior accumulation.

3.2.4. Scanning Electron Microscopy (SEM) characterization

SEM was used to study the surface morphology of MWCNTc and TLa-MWCNTc. The images from SEM are shown in Fig. 4.

Figure 4A(1-3) shows SEM images of glassy carbon surfaces modified with MWCNTc, while Fig. 4B(1-3) shows images of glassy carbon surfaces modified with TLa-MWCNTc. Comparison images with different magnifications are shown for both surfaces: 1) 4.43 KX (3µm), B) 24 KX 3µm and 52.61 KX (300nm).

When GCE is modified with the dispersion of MWCNTc, the surface is completely covered with MWCNTc, although the coverage is layered with different terraces, planes, and domains, where it can be seen that the surface is not flat and the aggregates can be observed in different areas. The addition of TLa leads to a very uniform and homogeneous distribution of the deposit, the size of the domains increases and shows less pronounced areas and a flattened and more homogeneous topography. From the comparison of Figures 4A3 and 4B3, it is clear that the CNTs modified with TLa are thicker and more dispersed due to the coating of CNTs with H-NADES, which is responsible for breaking the interactions between CNTs to create and enhance the dispersion of the nanomaterial, in contrast to what was observed for MWCNTc dispersion. Thus, the presence of TLa is critical for complete and homogeneous coverage of the GCE surface.

The homogeneous morphology of TLa-MWCNTc/GCE can improve the surface contact area with the product of enzymatic reaction while enabling fast electronic transfer for electrochemical reactions.

Journal Pre-proof

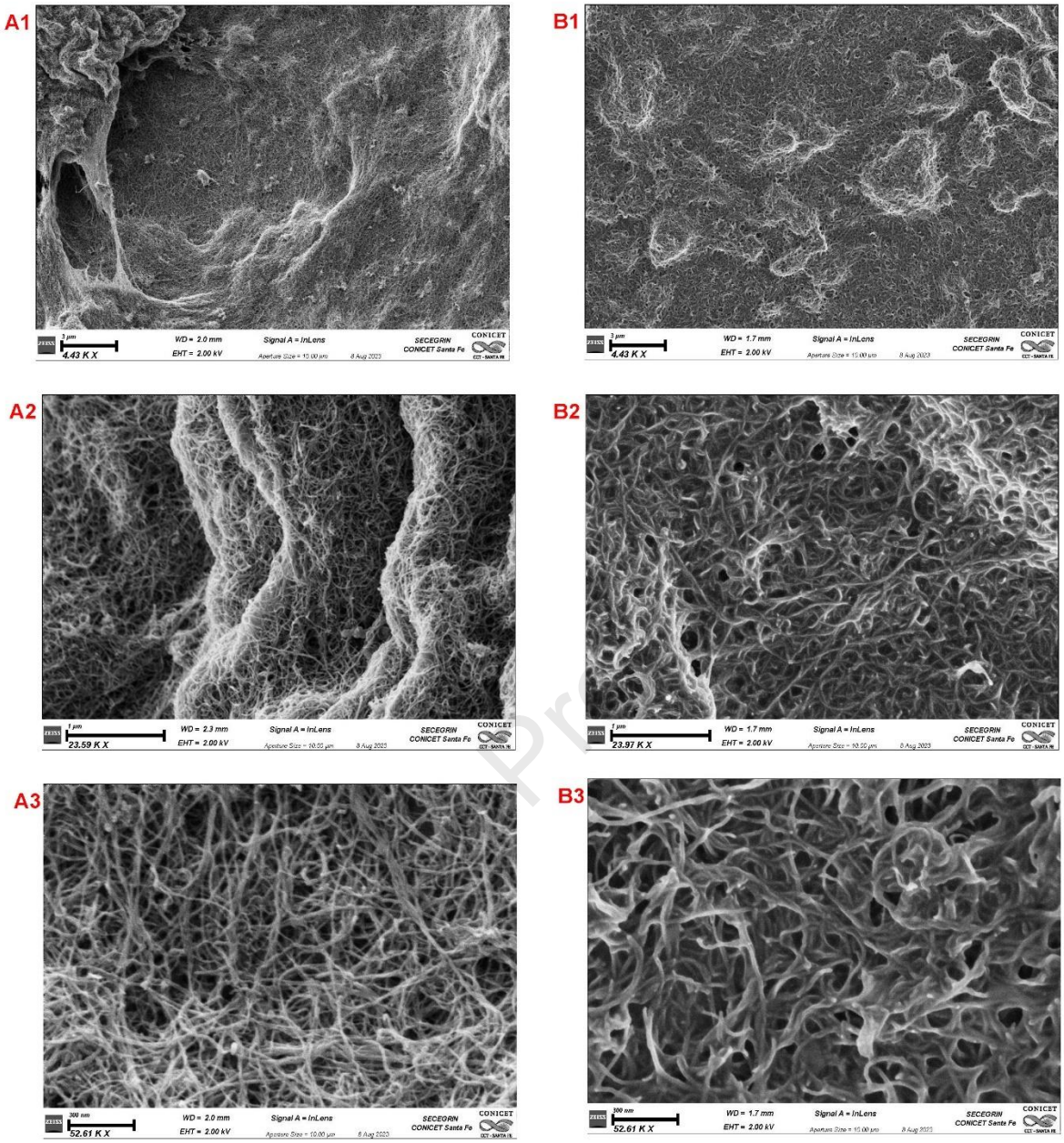

Figure 4. A) shows SEM images of glassy carbon surfaces modified with MWCNTc and B) TLa-MWCNTc. Comparative images with different magnifications are shown for both surfaces: 1) 4.43 KX (3um), B) 24 KX 3um and 52.61 KX (300nm).

3.2.5. UV-Vis

Figure SM4 show the spectra of a solution of thymol at 5%, TLa at 5%, MWCNTc dispersion and TLa-MWCNTc dispersion.

In the MWCNTc dispersion, congruently, an absorbance peak appears at 265 nm, due to the individual nanotubes strongly absorb at 265 nm due to the π-π* transition of aromatic sp^2

and the increase of the absorbance given by the dispersion of the CNT aggregates [38-41]. For thymol solution, a characteristic band is observed at 293 nm, which is present both in the TLa and in the TLa-MWCNTc dispersion. Additionally, a slight shoulder at approximately 265 nm is also observed in TLa-MWCNTc dispersion, due to the π-π* transition of aromatic sp^2 from carbon nanotubes, this signal is not observed in thymol and TLa solutions, concluding the presence of TLa and MWCNTc in the dispersion used to modified the vitreous carbon electrodes to build the sensor platform. Moreover, the ultrasonic treatment to which they are subjected does not greatly modify their natures.

3.3. Analytical performance

To define the linear range and the detection limit, a calibration curve was made varying on the sensor platform TLa-MWCNTc/GCE. Figure 5 represents the calibration plot between the value of peak current at 0.100 V corresponding to oxidation of the hydroxyl group of the *p*-NP generated by enzymatic cleavage and different α-glucosidase concentrations (from 0.004 to 0.8 U mL^{-1}). After the analysis, the linear range of the electrochemical method corresponds to 0.004 to 0.10 U mL^{-1}. In these conditions, the LOD and LOQ resulted 0.0013 and 0.0035 U mL^{-1}, respectively (see Table SM3). Furthermore, a comparison was made with the spectroscopic enzyme assays, and it was found that the linear range corresponded to the same obtained by the electrochemical method, but with higher LOD and LOQ (0.0019 and 0.0054 U mL^{-1}, respectively).

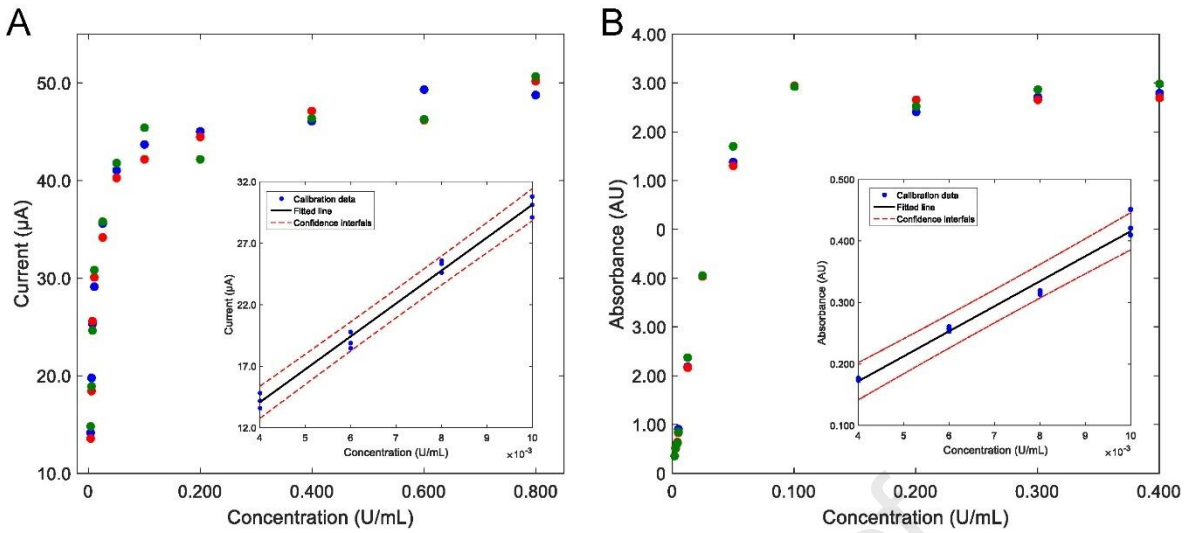

Figure 5. Plots of Peak current *vs* concentration of α-glucosidase: A) electrochemical method and B) reference method. The insert corresponds to the linear range in each case.

3.4. Determination of the activity of α-glucosidase

The activity of α-glucosidase was firstly investigated on the TLa-MWCNTc/GCE. A comparison between the analytical performance of the present method and those reported in the literature is shown in Table 1.

Journal Pre-proof

Table 1. A comparative of the method with previously reported ones.

System	Sample	Inhibitors	Detection limit (U mL^{-1})	Reusability	Reference
AuNPs modified with ATP aptamer and pAPG	Cell lysates. IPEC-J2 cell	3-propylidenephthalide	0.005	Yes – five times	[14]
AgNPs/DA and MNPs/pAPG with PBA/GE	Cell medium. IPEC-J2cells	Gallic acid and quercetin	0.1	No	[42]
CNHs/GCE	Mulberry bark extracts	Acarbose	0.00056	Yes – ten times	[43]
MWCNTs-α-glucosidase-PNPG-PVA	Tebengau (*Ehretis laevis*), Cemumar (*Micromelum pubescens*), and Kedondong (*Spondias dulcis*) plant leaves	Acarbose	5	No	[5]
TLa-MWCNTc/GCE		Acarbose, quercetin, gallic acid and rutin	0.0013	Yes – at least 15 times	The present work

AuNPs: gold nanoparticles; AgNPs: sliver nanoparticles; pAPG: 4-aminophenyl-α-d-glucopyranoside; MNPs: magnetic nanoparticles; PBA: pyrene boric acid; PVA: freeze-thawed polyvinyl alcohol; PNPG: *p*-nitrophenyl-α-D-glucopyranoside; GE: graphite electrode; GCE: glassy carbon electrodes; CNH: carbon nanohorns; MWCNTc: Carboxylic Multi-walled carbon nanotubes; MWCNT: Multi-walled carbon nanotubes

Journal Pre-proof

Journal Pre-proof

The results show that the proposed method has an excellent detection limit (see Table SM3). It is important to note that most of the results shown in Table 1, are mostly less sensitive than the present method, i.e., the TLa-MWCNTc/GCE method presents LOD better than the other reported methods [5, 14, 42]. Another remarkable fact is that the sensor was reused at least 15 times, resulting in an excellent option for a routine analysis.

Moreover, during the validation, the development method was compared with the reference methos (spectrophotometric enzyme assay). In this sense, only in this work, a complete verification of the data obtained by the electrochemical sensor *vs* the reference was performed. This comparison clearly shows that the reported sensor has one of the most competitive performances and offers many advantages for the determination of α-glucosidase and its inhibitors, such as the simplicity of electrode preparation, not only in terms of sensitivity and detection limits achieved, but also in terms of average reproducibility and repeatability.

3.5. Measurement of the inhibitory activities of the synthetic drug (acarbose) and quercetin by DPV.

In order to demonstrate the practicability of the developed method to screen α-glucosidase inhibitors, two compounds (acarbose and quercetin) have been chosen. In the presence of inhibitors, the enzymatic reaction between the *p*-NPG and α-glucosidase exhibits a lower peak current of released *p*-NP. Acarbose, which is a common anti-diabetes drug and along with quercetin which is probably one of the major components of plant extracts were selected as the examples to evaluate the ability of screening α-glucosidase inhibitors. As result, increasing acarbose concentration from 0.05 to 8.00 mM, the oxidation peak currents of hydroxyl group gradually decreased showing the ability of acarbose to inhibit enzyme activity. In Fig. SM5A, the inhibition effect of acarbose on α-glucosidase activity can be observed. The maximum

inhibition of acarbose is 86% with an IC50 value of (3 ± 1) mM, and it has been reported that acarbose is a competitive inhibitor of α-glucosidase [34]. Figure SM5B shows the inhibition effect of quercetin in the range from 0.004 to 1.0 mM on α-glucosidase activity. For quercetin, the maximum inhibition ratio is 99% with an IC50 value of (0.015 ± 0.004) mM. Different from acarbose, quercetin can noncompetitively and anticompetitively inhibit α-glucosidase activity [44, 45].

During the validation, studies of the inhibition effect of quercetin were also carried out using spectrophotometric enzyme assays (Fig. SM5B). Due to quercetin presents a yellow coloration, values greater than 0.10 mM cannot be detected by the spectrophotometric assay, presenting the maximum detectable inhibition ratio as 75% with the IC50 value of (0.011 ± 0.003) mM.

As a result, the electrochemical method is more sensitive for measuring the antidiabetic potential of medicinal plants than the colorimetric method. These facts confirm that the proposed method can be successfully used for the inhibitor screening in the medium containing the enzyme.

3.6. Study of the inhibitory activities of plant extracts by electrochemical method

To define the use of the present method in real samples, the analysis of the feasibility of the use of plant extract as inhibitor was carried out. The experiments were carried out using concentrations of *p*-NPG and α-glucosidase at 1.00 mM and 0.05 U mL^{-1}, respectively.

Moreover, to verify the specificity of the present method *vs* the reference inhibitory capacity of the extracts, they were determined by spectrophotometric enzyme assays. Figure 5A shows a photo of the spectrophotometric enzyme assays microplates for the different inhibition assays.

Two different plants extracts (*Schinus m.* and *Eugenia u.*) (from 1.52 to 400 µg mL^{-1}) were used to measure the inhibition potential through DPV on TLa-MWCNTc/GCE using the equation by Eq. 1 to obtain a result.

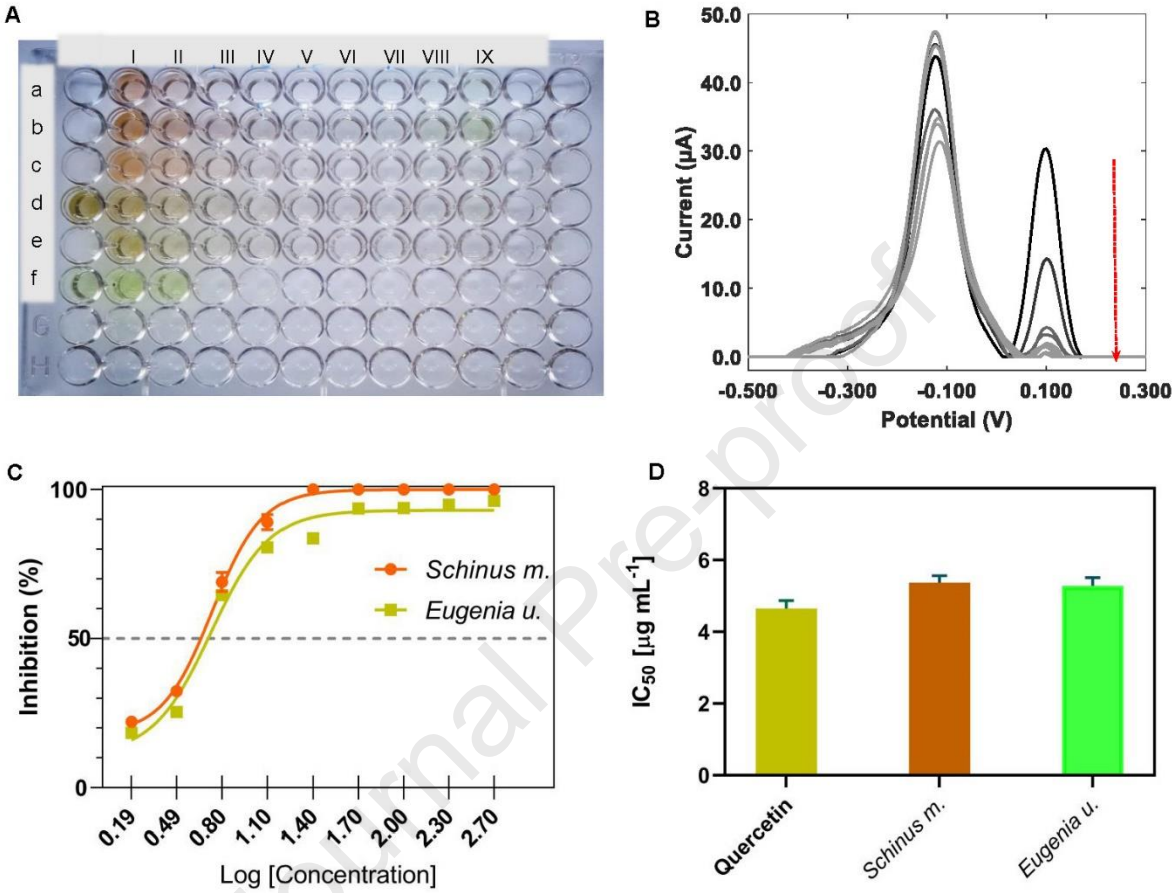

Figure 6. A) Photograph of a 96-well microplate used for the spectrophotometric assays to determine the inhibition of glucosidase. The line (a) and (b), correspond to *Schinus molle* extract at different concentrations (1.52 to 400 µg mL^{-1}) with enzyme and substrate (n = 2); (c) correspond to *Schinus molle* extract as blank at the same concentration as above. (d) correspond to *Eugenia uniflora* extract at different concentrations (1.52 to 400 µg mL^{-1}) with enzyme and substrate and (e) correspond to the blank. The line (f) corresponds to the control (without inhibitor) (n = 3). Increasing concentrations correspond to columns I to IX (in descending order). B) Differential pulse voltammograms of 1.00 mM *p*-NPG with 0.05 U mL^{-1} α-glucosidase in the presence of different concentrations of *Eugenia u.* (extracts) (from 1.52 to 400 µg mL^{-1}) in 0.100 M PB (pH = 6.8) on the TLa-MWCNTc/GCE. C) Inhibitory effect of *Eugenia u.* and *Schinus m.* extracts ranging from 1.52 to 400 µg mL^{-1} on α-glucosidase activity. x-axis in log [concentration]. D) Comparative graph of IC50 values between quercetin and the studied plant extracts. All measurements were performed with a concentration of *p*-NPG and α-glucosidase of 1.00 mM and 0.05 U mL^{-1}, respectively.

Journal Pre-proof

510 The corresponding plots in Fig. 6B show that the increase in the extract concentration of
511 *Eugenia uniflora* generates an inhibition increase, as a consequence of the signal decrease
512 associated with the oxidation of the released *p*-NP hydroxyl group. The maximum inhibition
513 of *Schinus molle* extract was (91 ± 3) % for a concentration of 12.5 μg mL^{-1} with the IC50
514 value of 5.37 μg mL^{-1}, the inhibited released *p*-NP. For the *Eugenia uniflora* extract, the
515 maximum inhibition was (81 ± 2) % for a concentration of 12.5 μg mL^{-1} and the IC50 was 5.28
516 μg mL^{-1} (Fig. 6C).

517 In presence of plant extracts, the enzymatic reaction between the *p*-NPG and α-glucosidase
518 exhibits a lower peak current of released *p*-NP, that is, when the extract was added as an
519 inhibitor, the oxidation peak currents of the released *p*-NP decreased as compared to those of
520 the control (Fig. 6B).

521 During the analysis by spectrophotometric enzyme assays, as the extracts are colored, the
522 inhibitory capacity of the extracts cannot be determined, since a clear interference is observed,
523 so the curves lose sensitivity and there are also several concentrations in which the
524 measurements are not detectable. Therefore, the developed electrochemical method is
525 appropriate and highly sensitive and selective to determine inhibition in complex and colored
526 samples.

527 Figure 6D shows the comparison of the IC50 values of the inhibitor's quercetin and the
528 extracts of *Schinus molle* and *Eugenia uniflora*, it can be seen that the extracts present higher
529 inhibitor efficiency.

530 The above discussion clearly shows that the TLa-MWCNTc/GCE sensor platform be used
531 for sensitively detecting α-glucosidase activity and screening the anti-diabetic drug and but
532 also suggests that the sensor is suitable for the monitoring of antidiabetic potential compounds
533 present in plants as well as the synthetic commercial drugs.

534

3.7. Selectivity, reproducibility and reusability of the proposed sensor.

First, the different extracts were measured with the sensor platform under the test conditions and no analytical signals were observed in the potential range studied, so the extracts do not present components that could interfere with the analytical signal under study. In addition, several potential interfering compounds including various metal ions (K^+, Ca^{2+}, Na^+, Mg^{2+} and Fe^{3+}) and common amino acids as well as simple and complex carbohydrates (glucose, fructose, dextrose and sucrose) were investigated by DPV under the same conditions. The possible interferents were separately added into a reaction solution containing 1.00 mM *p*-NPG and 0.05 U mL^{-1} α-glucosidase and a final concentration of 2 mM, which is 2 and 250 times than the minimum concentration of acarbose and quercetin that shows inhibition. As result, these compounds did not show an effect on the inhibitory efficiency (data not shown).

Therefore, the result demonstrates that the developed detection methods based on TLa-MWCNTc/GCE possess excellent selectivity towards α-glucosidase inhibitor, owing to high inhibition of acarbose and quercetin towards α-glucosidase activity.

Moreover, the reproducibility and stability of the electrochemical sensor were investigated. A series of 6 modified electrodes were prepared under the same conditions to evaluate the reproducibility of this sensor and the relative standard deviation (RSD) was 7.1%, suggesting a good reproducibility.

The reusability of the fabricated sensor was studied through at least 15 successive DPV measurements. As result, the variability of the peak current of *p*-NP was least than 5%, which suggested an excellent reusability of our proposed sensor. The above results proved that the present electrochemical sensor has a good reproducibility and reusability.

4. Conclusions

In this work, we have fabricated a reusable, stable, and simple electrochemical sensor based on carbon nanotube and hydrophobic NADES-modified glassy carbon electrode to detect activity assay, inhibitor screening and screening of potential anti-diabetic medicine.

The use of TLa is proposed for the first time and in an innovative way to disperse carbon nanostructures, fulfilling two fundamental roles, dispersing nanomaterials and increasing their electrochemical response.

The applicability of the method has also been confirmed by the results obtained from detection of the extracts of *Schinus molle* and *Eugenia uniflora* and different commercial inhibitors with high sensitivity and selectivity. It was also validated by the reference method (spectrophotometric enzyme assays) widely showing the superior efficiency, accuracy and confidence of the developed method, it presents several advantages compared to the reference spectroscopic method, in terms of linear range, LOD and interference in detection, it can be used to measure colored interferents and complex matrices.

Acknowledgments

The authors are grateful to ANPCyT (Agencia Nacional de Promoción Científica y Tecnológica, Projects PICT 2020-0105, 2020-0304 and 2021-0029) for financial support.

Journal Pre-proof

578 **Figure captions**

579 **Figure 1.** Response surface countour plot for the combined central composite design (CCD).
580 The plot described the %H-NADES vs Potential when the other parameters are fixed at the
581 optimum conditions.
582

583 **Figure 2.** A) Reaction scheme of hydrolysis of colourless p-nitrophenyl-α-d-glucopyranoside
584 to coloured p-nitrophenol by α-glucosidase. B) Differential pulse voltammograms of 1.00 mM
585 *p*-NP in 0.100 M PB (pH = 6.8) on the GCE (blue dotted line), TLa/GCE (yellow dash-dotted
586 line) MWCNTc/GCE (red dots) and TLa-MWCNTc/GCE (violet solid line). Right inset:
587 shown the voltammetric profile (DPV) obtained before subtracting background currents. Left
588 insert: the DPVs of GCE (blue dotted line), and MWCNTc/GCE (yellow dash-dotted line) were
589 magnified. Potential range of −0.4 V to 0.3 V. The voltammetric profiles were obtained after
590 subtracting background currents.
591

592 **Figure 3.** Shows the variation of the potential and current of the peak associated with the
593 oxidation of the hydroxyl group of the *p*-NP generated on different surfaces, GCE, TLa/GCE,
594 MWCNTc/GCE and TLa-MWCNTc/GCE
595

596 **Figure 4.** A) shows SEM images of glassy carbon surfaces modified with MWCNTc and B)
597 TLa-MWCNTc. Comparative images with different magnifications are shown for both
598 surfaces: 1) 4.43 KX (3um), B) 24 KX 3um and 52.61 KX (300nm).
599

600 **Figure 5.** Plots of Peak current *vs* concentration of α-glucosidase: A) electrochemical method
601 and B) reference method. The insert corresponds to the linear range in each case.
602

603 **Figure 6.** A) Photograph of a 96-well microplate used for the spectrophotometric assays to
604 determine the inhibition of glucosidase. The line (a) and (b), correspond to *Schinus molle*
605 extract at different concentrations (1.52 to 400 µg mL^{-1}) with enzyme and substrate (n = 2); (c)
606 correspond to *Schinus molle* extract as blank at the same concentration as above. (d) correspond
607 to *Eugenia uniflora* extract at different concentrations (1.52 to 400 µg mL^{-1}) with enzyme and
608 substrate and (e) correspond to the blank. The line (f) corresponds to the control (without
609 inhibitor) (n = 3). Increasing concentrations correspond to columns I to IX (in descending
610 order). B) Differential pulse voltammograms of 1.00 mM *p*-NPG with 0.05 U mL^{-1} α-
611 glucosidase in the presence of different concentrations of *Eugenia u.* (extracts) (from 1.52 to
612 400 µg mL^{-1}) in 0.100 M PB (pH = 6.8) on the TLa-MWCNTc/GCE. C) Inhibitory effect of
613 *Eugenia u.* and *Schinus m.* extracts ranging from 1.52 to 400 µg mL^{-1} on α-glucosidase activity.
614 x-axis in log [concentration]. D) Comparative graph of IC50 values between quercetin and the
615 studied plant extracts. All measurements were performed with a concentration of *p*-NPG and
616 α-glucosidase of 1.00 mM and 0.05 U mL^{-1}, respectively.
617

618

619

620

621

622 **References**

623 [1] I.D. Federation, IDF Diabetes Atlas, 8th ed.2017.
624 [2] A.D. Seetaloo, M.Z. Aumeeruddy, R.R. Rengasamy Kannan, M.F. Mahomoodally, Potential
625 of traditionally consumed medicinal herbs, spices, and food plants to inhibit key digestive
626 enzymes geared towards diabetes mellitus management — A systematic review, S. Afr. J. Bot.
627 120 (2019) 3-24. https://doi.org/10.1016/j.sajb.2018.05.015.
628 [3] X. Huang, K.S.E. Tanaka, A.J. Bennet, Glucosidase-Catalyzed Hydrolysis of α-d-
629 Glucopyranosyl Pyridinium Salts: Kinetic Evidence for Nucleophilic Involvement at the
630 Glucosidation Transition State, J. Am. Chem. Soc. 119(46) (1997) 11147-11154.
631 https://doi.org/10.1021/ja963733l.
632 [4] C. Hansawasdi, J. Kawabata, Alpha-glucosidase inhibitory effect of mulberry (*Morus alba*)
633 leaves on Caco-2, Fitoterapia 77(7-8) (2006) 568-73.
634 https://doi.org/10.1016/j.fitote.2006.09.003.
635 [5] M. Mohiuddin, D. Arbain, A.K.M.S. Islam, M.S. Ahmad, M.N. Ahmad, Alpha-Glucosidase
636 Enzyme Biosensor for the Electrochemical Measurement of Antidiabetic Potential of Medicinal
637 Plants, Nanoscale Res. Lett. 11(1) (2016) 95. https://doi.org/10.1186/s11671-016-1292-1.
638 [6] J. Zhang, Y. Liu, J. Lv, G. Li, A colorimetric method for α-glucosidase activity assay and its
639 inhibitor screening based on aggregation of gold nanoparticles induced by specific recognition
640 between phenylenediboronic acid and 4-aminophenyl-α-d-glucopyranoside, Nano Res. 8(3)
641 (2015) 920-930. https://doi.org/10.1007/s12274-014-0573-1.
642 [7] J.H. Kim, Y.B. Ryu, N.S. Kang, B.W. Lee, J.S. Heo, I.Y. Jeong, K.H. Park, Glycosidase inhibitory
643 flavonoids from Sophora flavescens, Biol Pharm Bull 29(2) (2006) 302-5. 10.1248/bpb.29.302.
644 [8] H. Liu, P. He, Z. Li, C. Sun, L. Shi, Y. Liu, G. Zhu, J. Li, An ionic liquid-type carbon paste
645 electrode and its polyoxometalate-modified properties, Electrochem. Commun. 7(12) (2005)
646 1357-1363. https://doi.org/10.1016/j.elecom.2005.09.018.
647 [9] H. Parham, N. Rahbar, Square wave voltammetric determination of methyl parathion using
648 ZrO2-nanoparticles modified carbon paste electrode, J. Hazard. Mater. 177(1) (2010) 1077-
649 1084. https://doi.org/10.1016/j.jhazmat.2010.01.031.
650 [10] T. Matsui, C. Yoshimoto, K. Osajima, T. Oki, Y. Osajima, In vitro survey of alpha-glucosidase
651 inhibitory food components, Biosci Biotechnol Biochem 60(12) (1996) 2019-22.
652 https://doi.org/10.1271/bbb.60.2019.
653 [11] Y. Sawada, T. Tsuno, T. Ueki, H. Yamamoto, Y. Fukagawa, T. Oki, Pradimicin Q, a new
654 pradimicin aglycone, with alpha-glucosidase inhibitory activity, J Antibiot (Tokyo) 46(3) (1993)
655 507-10. https://doi.org/10.7164/antibiotics.46.507.
656 [12] A. Cao, Y. Tang, Y. Liu, Novel Fluorescent Biosensor for α-Glucosidase Inhibitor Screening
657 Based on Cationic Conjugated Polymers, ACS Appl. Mater. Interfaces 4(8) (2012) 3773-3778.
658 https://doi.org/10.1021/am3010913.
659 [13] J. Zhang, Y. Liu, X. Wang, Y. Chen, G. Li, Electrochemical assay of α-glucosidase activity and
660 the inhibitor screening in cell medium, Biosens Bioelectron 74 (2015) 666-72.
661 https://doi.org/10.1016/j.bios.2015.07.023.
662 [14] J. Li, G. He, B. Wang, L. Shi, T. Gao, G. Li, Fabrication of reusable electrochemical biosensor
663 and its application for the assay of α-glucosidase activity, Anal. Chim. Acta 1026 (2018) 140-
664 146. https://doi.org/10.1016/j.aca.2018.04.015.
665 [15] Y.-Y. Liu, H. Li, L. Lu, B. Sun, L. Huang, H. Chen, W. Qiu, J. Tao, P. Zhao, A Ratiometric
666 Electrochemical Sensor with Integrated Probe for the Assay of α-glucosidase Activity and
667 Screening of Its Inhibitors, J. Electrochem. Soc. 166 (2) (2019) B133-B140.
668 https://doi.org/10.1149/2.1111902jes.
669 [16] Y. Jian-Ping, Z. Cai-Jun, L. Qiu-Na, C. Hua-Ying, H. Zhi-Xuan, L. Zhi-Kang, L. Xiao, L. Nan-
670 Feng, A Novel Method for Screening α-Glycosidase Inhibitors Based on Nickel-based

671 Nanomaterial Electrochemical Sensor, J. Chin. Chem. Soc. (2023) 372 - 382.
672 https://doi.org/10.19756/j.issn.0253-3820.22100.
673 [17] S.B. Hočevar, I. Švancara, K. Vytřas, B. Ogorevc, Novel electrode for electrochemical
674 stripping analysis based on carbon paste modified with bismuth powder, Electrochim. Acta
675 51(4) (2005) 706-710. https://doi.org/10.1016/j.electacta.2005.05.023.
676 [18] Y. Wang, Y. Wu, J. Xie, X. Hu, Metal–organic framework modified carbon paste electrode
677 for lead sensor, Sens. Actuators, B 177 (2013) 1161-1166.
678 https://doi.org/10.1016/j.snb.2012.12.048.
679 [19] Y. Wang, T. Wu, C.-y. Bi, Simultaneous determination of acetaminophen, theophylline and
680 caffeine using a glassy carbon disk electrode modified with a composite consisting of
681 poly(Alizarin Violet 3B), multiwalled carbon nanotubes and graphene, Microchim. Acta 183(2)
682 (2016) 731-739. https://doi.org/10.3390/app810192510.1007/s00604-015-1688-0.
683 [20] U.G. Sauer, A. Aumann, L. Ma-Hock, R. Landsiedel, W. Wohlleben, Influence of dispersive
684 agent on nanomaterial agglomeration and implications for biological effects in vivo or in vitro,
685 Toxicol In Vitro 29(1) (2015) 182-6. https://doi.org/10.1016/j.tiv.2014.10.011.
686 [21] L.Q. Hoa, M.d.C. Vestergaard, H. Yoshikawa, M. Saito, E. Tamiya, Functionalized multi-
687 walled carbon nanotubes as supporting matrix for enhanced ethanol oxidation on Pt-based
688 catalysts, Electrochem. Commun. 13(7) (2011) 746-749.
689 https://doi.org/10.1016/j.elecom.2011.03.041.
690 [22] A.C. Zaman, C.B. Üstündağ, F. Kaya, C. Kaya, OH and COOH functionalized single walled
691 carbon nanotubes-reinforced alumina ceramic nanocomposites, Ceram. Int. 38(2) (2012) 1287-
692 1293. https://doi.org/10.1016/j.ceramint.2011.09.002.
693 [23] K. Zhang, J.Y. Lim, H.J. Choi, Amino functionalization and characteristics of multi-walled
694 carbon nanotube/poly(methyl methacrylate) nanocomposite, Diamond Relat. Mater. 18(2)
695 (2009) 316-318. https://doi.org/10.1016/j.diamond.2008.08.005.
696 [24] A. Gałuszka, Z. Migaszewski, J. Namieśnik, The 12 principles of green analytical chemistry
697 and the SIGNIFICANCE mnemonic of green analytical practices, TrAC, Trends Anal. Chem. 50
698 (2013) 78-84. https://doi.org/10.1016/j.trac.2013.04.010.
699 [25] Á. Santana-Mayor, R. Rodríguez-Ramos, A.V. Herrera-Herrera, B. Socas-Rodríguez, M.Á.
700 Rodríguez-Delgado, Deep eutectic solvents. The new generation of green solvents in analytical
701 chemistry, TrAC, Trends Anal. Chem. 134 (2021) 116108.
702 https://doi.org/10.1016/j.trac.2020.116108.
703 [26] B.D. Ribeiro, C. Florindo, L.C. Iff, M.A.Z. Coelho, I.M. Marrucho, Menthol-based Eutectic
704 Mixtures: Hydrophobic Low Viscosity Solvents, ACS Sustainable Chem. Eng. 3(10) (2015) 2469-
705 2477. https://doi.org/10.1021/acssuschemeng.5b00532.
706 [27] F.J.V. Gomez, M. Espino, M. de los Angeles Fernandez, J. Raba, M.F. Silva, Enhanced
707 electrochemical detection of quercetin by Natural Deep Eutectic Solvents, Anal. Chim. Acta 936
708 (2016) 91-96. https://doi.org/10.1016/j.aca.2016.07.022.
709 [28] S.M. Azcarate, R. Elia Dazat, J.M. Camiña, M.F. Silva, F.J.V. Gomez, NADES-modified
710 voltammetric sensors and information fusion for detection of honey heat alteration, Food
711 Control 140 (2022) 109144. https://doi.org/10.1016/j.foodcont.2022.109144.
712 [29] A. Sherlin V, X.B. Joseph, S.-F. Wang, J.N. Baby, M. George, Natural deep eutectic solvent
713 assisted synthesis of FeMnO3 entrapped functionalized carbon nanofiber composite: An
714 electrochemical detection of nimesulide, J. Mol. Liq. 367 (2022) 120421.
715 https://doi.org/10.1016/j.molliq.2022.120421.
716 [30] V. Selvanathan, A.D. Azzahari, A.A. Abd. Halim, R. Yahya, Ternary natural deep eutectic
717 solvent (NADES) infused phthaloyl starch as cost efficient quasi-solid gel polymer electrolyte,
718 Carbohydr. Polym. 167 (2017) 210-218. https://doi.org/10.1016/j.carbpol.2017.03.023.
719 [31] C.M. Teglia, F.A. Gutierrez, H.C. Goicoechea, Natural deep eutectic solvent: A novelty
720 alternative as multi-walled carbon nanotubes dispersing agent for the determination of
721 paracetamol in urine, Talanta 242 (2022) 123290.
722 https://doi.org/10.1016/j.talanta.2022.123290.

[32] L. Vera Candioti, M.M. De Zan, M.S. Cámara, H.C. Goicoechea, Experimental design and multiple response optimization. Using the desirability function in analytical methods development, Talanta 124 (2014) 123-138. https://doi.org/10.1016/j.talanta.2014.01.034.
[33] R.E. Dazat, S.B. Mammana, B.V. Canizo, M.F. Silva, F.J.V. Gomez, Enhanced fluorescence detection of ergosterol by hydrophobic fluorescent natural deep eutectic solvent, Green Anal. Chem. 3 (2022) 100026. https://doi.org/10.1016/j.greeac.2022.100026.
[34] BRENDA:EC3.2.1.20, Information on EC 3.2.1.20 - alpha-glucosidase and Organism(s) Saccharomyces cerevisiae. https://www.brenda-enzymes.org/enzyme.php?ecno=3.2.1.20&Suchword=&reference=&UniProtAcc=&organism%5B%5D=Saccharomyces+cerevisiae&show_tm=0#REF.
[35] J. Feng, X.W. Yang, R.F. Wang, Bio-assay guided isolation and identification of α-glucosidase inhibitors from the leaves of Aquilaria sinensis, Phytochemistry 72(2-3) (2011) 242-7. https://doi.org/10.1016/j.phytochem.2010.11.025.
[36] S.A. Gegenschatz, F.A. Chiappini, C.M. Teglia, A. Muñoz de la Peña, H.C. Goicoechea, Binding the gap between experiments, statistics, and method comparison: A tutorial for computing limits of detection and quantification in univariate calibration for complex samples, Anal. Chim. Acta (2021) 339342. https://doi.org/10.1016/j.aca.2021.339342.
[37] B. Elya, K. Basah, A. Mun'im, W. Yuliastuti, A. Bangun, E.K. Septiana, Screening of α-glucosidase inhibitory activity from some plants of Apocynaceae, Clusiaceae, Euphorbiaceae, and Rubiaceae, J Biomed Biotechnol 2012 (2012) 281078. https://doi.org/10.1155/2012/281078.
[38] Y. Liu, L. Yu, S. Zhang, J. Yuan, L. Shi, L. Zheng, Dispersion of multiwalled carbon nanotubes by ionic liquid-type Gemini imidazolium surfactants in aqueous solution, Colloids Surf., A 359(1) (2010) 66-70. https://doi.org/10.1016/j.colsurfa.2010.01.065.
[39] Z. Wu, W. Feng, Y. Feng, Q. Liu, X. Xu, T. Sekino, A. Fujii, M. Ozaki, Preparation and characterization of chitosan-grafted multiwalled carbon nanotubes and their electrochemical properties, Carbon 45(6) (2007) 1212-1218. https://doi.org/10.1016/j.carbon.2007.02.013.
[40] J. Yu, N. Grossiord, C.E. Koning, J. Loos, Controlling the dispersion of multi-wall carbon nanotubes in aqueous surfactant solution, Carbon 45(3) (2007) 618-623. https://doi.org/10.1016/j.carbon.2006.10.010.
[41] F. Lu, S. Zhang, L. Zheng, Dispersion of multi-walled carbon nanotubes (MWCNTs) by ionic liquid-based phosphonium surfactants in aqueous solution, J. Mol. Liq. 173 (2012) 42-46. https://doi.org/10.1016/j.molliq.2012.06.012.
[42] J. Zhang, Y. Liu, X. Wang, Y. Chen, G. Li, Electrochemical assay of α-glucosidase activity and the inhibitor screening in cell medium, Biosens. Bioelectron. 74 (2015) 666-672. https://doi.org/10.1016/j.bios.2015.07.023.
[43] Y. Liu, H. Li, L. Lu, B. Sun, L. Huang, H. Chen, W. Qiu, J. Tao, P. Zhao, A Ratiometric Electrochemical Sensor with Integrated Probe for the Assay of α-glucosidase Activity and Screening of Its Inhibitors, J. Electrochem. Soc. 166(2) (2019) B133. https://doi.org/10.1149/2.1111902jes.
[44] Y.Q. Li, F.C. Zhou, F. Gao, J.S. Bian, F. Shan, Comparative Evaluation of Quercetin, Isoquercetin and Rutin as Inhibitors of α-Glucosidase, J. Agric. Food. Chem. 57(24) (2009) 11463-11468. https://doi.org/10.1021/jf903083h.
[45] D. Roncancio, H. Yu, X. Xu, S. Wu, R. Liu, J. Debord, X. Lou, Y. Xiao, A Label-Free Aptamer-Fluorophore Assembly for Rapid and Specific Detection of Cocaine in Biofluids, Anal Chem 86(22) (2014) 11100-11106. https://doi.org/10.1021/ac503360n.

Journal Pre-proof

Highlights

►First time of MWCNTc and H-NADES based electrochemical sensor for of α-glucosidase and its inhibitors determination.

►The sensor shows impressive electro-catalytic activity towards enzymatic reaction.

►Successful estimation of commercial α-glucosidase inhibitors and plant extracts as potential antidiabetic drugs.

►The sensor is highly stable and reproducible.

Journal Pre-proof

Journal Pre-proof

Declaration of interests

☒ The authors declare that they have no known competing financial interests or personal relationships that could have appeared to influence the work reported in this paper.

☐The authors declare the following financial interests/personal relationships which may be considered as potential competing interests:

Journal Pre-proof